

# SPACE DEBRIS WITH HIGH A/M: A WEB OF SUB-RESONANCES

Delsate. N.<sup>(1)</sup> and Lemaître. A.<sup>(2)</sup>

<sup>(1,2)</sup>University of Namur (FUNDP), Department of Mathematics, Rempart de la Vierge 8, B-5000 Namur, Belgium.  
E-mail<sup>(1)</sup> : nicolas.delsate@math.fundp.ac.be      E-mail<sup>(2)</sup> : anne.lemaitre@fundp.ac.be

## ABSTRACT

The dynamics of space debris with very high  $A/m$  near the geostationary orbit is dominated by the gravitational coefficient  $C_{22}$  and the solar radiation pressure. We propose a stability atlas, for a large set of these objects, by numerically computing a diffusion indicator (using FMA). The results show chaotic layers around the separatrix and a relevant class of secondary resonances (associated to the period of the sun) near the pendulum-like pattern of geostationary objects. This succession of stable and chaotic layers can be reproduced and explained by a simple toy model, based on a pendulum approach, perturbed, through the eccentricity, by the Sun frequency. The use of action-angle variables in the circulation and libration regions of the pendulum allows to point out new resonances between the geostationary libration angle and the Sun's longitude.

Key words: Geostationary; Space debris; Secondary resonance; Analytical model; Solar radiation pressure.

## 1. INTRODUCTION

Recent optical surveys in high-altitude orbits, performed by the European Space Agency 1 m telescope on Tenerife (Canary islands), have shown a new unexpected population of 10 cm size space debris near the geostationary region (GEO). The dynamics of these objects can be strongly perturbed by the solar radiation pressure, if their coefficient "area to mass" ( $A/m$ ) is large (between 1 and 30 m<sup>2</sup>/kg), as suggested by Liou and Weaver [12]. In that case, the solar radiation pressure becomes the second acting force, after the central force. The dynamics of such geostationary objects has been analyzed by several authors, as Anselmo and Pardini [1], Liou and Weaver [13], Chao [3] or Valk et al. [16].

The stability of the near-geostationary region has been studied using the MEGNO chaos indicator [4, 5]: let us mention Breiter et al. [2] for low area-to-mass ratios and Valk et al. [17] for high area-to-mass ratios. Their results have been confirmed and refined, using the Frequency Map Analysis, Delsate et al. [6].

The analysis of the stability, using various numerical methods, brings to the fore the presence of a web of sub-structures, connected to periods of the resonant geostationary angle multiples of one year (resonances between the geostationary resonant angle and the longitude of the Sun), produced by this important solar radiation pressure. Formally the term *secondary resonances* is reserved for the libration region only, but we shall use it also to describe the resonances between the two angles in the outer and inner circulation regions.

These stable islands, even if they have small sizes, could be considered as potential reservoirs of debris of large  $A/m$  captured in these layers for some periods of time (several tens or hundreds of years).

In this proceedings, we present the numerical results of the Frequency Map Analysis (FMA) and the guideline of the toy model developed in [11]. This simplified model reproduces the main features of the numerical analysis of Delsate et al. [6] and explains how the two angles combine to give several new secondary resonances. We choose a sample case for  $A/m = 10$  meters<sup>2</sup>/kg. The model is a pendulum-like, averaged over the short periodic terms and perturbed by the solar radiation pressure through the eccentricity. The introduction of suitable couples of action-angle variables in the libration and circulation zones allows us to detect all the significative resonances and their respective positions, to find the sizes of the small islands and to give, for each of them, an suitable very local model of resonance.

The paper starts with a short description of the forces appear in the dynamics of GEO space debris, followed by the description and results of the FMA to end up with the description and the results of the perturbed pendulum approach.

## 2. MODELISATION AND RESULTS

Let us introduce the usual following notations:  $a$  for the semi-major axis,  $e$  for the eccentricity and  $i$  for the inclination of the small object as well as  $\lambda = M + \Omega + \omega$  for its mean longitude;  $\omega$  designates the argument of the pericenter,  $\Omega$  the longitude of the ascending node and  $M$  the mean anomaly. The angle  $\theta$  represents the rotation of the

Earth, considered as uniform. We define  $\sigma = \lambda - \theta$ , the mean longitude of the body in a Earth-rotating frame and  $\lambda_S$  is the longitude of the sun in a fixed frame (Fig. 1).

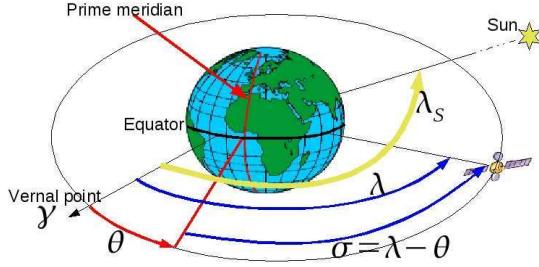


Figure 1. Geostationary resonant angle  $\sigma$  and sun longitude  $\lambda_S$  definitions.

For this study, we select the main forces that contribute to the dynamics of GEO space debris. The numerical model combines the second-order gravitational potential of the Earth, including  $J_2$ ,  $C_{22}$  and  $S_{22}$ , and the solar radiation pressure, with the Earth orbiting on an eccentric and inclined orbit around the Sun. The debris are supposed to be very close to the geostationary orbit and are characterized by the following initial conditions  $e = 0.002$ ,  $i = 0.22^\circ$ ,  $\Omega = \omega = 0^\circ$  and the initial time is 25 January 1991. The area-to-mass ratio is equal to 10 meters<sup>2</sup>/kg.

## 2.1. Numerical tools: Frequency Map Analysis

The FMA (Frequency Map Analysis) is a very efficient numerical method of frequency analysis [8, 9], much more efficient than a classical FFT. Indeed, for a KAM solution, the accuracy of the frequencies of a signal on a time span  $[-T, T]$  is proportional to  $1/T^4$  for the FMA, using a Hanning window [10], while for an ordinary FFT method, this accuracy is only proportional to  $1/T$ .

The main purpose of the FMA is to determine the approximation  $f'(t)$  of a signal  $f(t)$  where both functions are developed in Fourier series:

$$f'(t) = \sum_{k=1}^N p'_k e^{i\nu'_k t} \quad f(t) = \sum_{k=1}^{\infty} p_k e^{i\nu_k t}$$

The frequencies  $\nu'_k$  for  $k = 1, \dots, N$  and their associated decreasing amplitudes  $p'_k$  for  $k = 1, \dots, N$  are determined through an iterative scheme.

To estimate the time diffusion of the main frequency  $\nu_1$  with respect to the time, we compute a first value  $\nu_1^{(1)}$  of the main frequency of the signal on a first time span  $[-T, 0]$  and a second value  $\nu_1^{(2)}$  of this main frequency on a second time span  $[0, T]$ . We estimate the diffusion rate (noted EOD) of the frequency with respect to the time by the formula [9]:

$$\text{EOD} = \log \left( \frac{\nu_1^{(1)} - \nu_1^{(2)}}{\nu_1^{(1)}} \right).$$

Our study concerns the geostationary resonance area in which we study the variation of the main frequency (proper frequency) of the signal ( $a \cos \sigma, a \sin \sigma$ ). The results of this frequency analysis are reported in Fig. 2. Similarly results and complementary details and explanation have been published in Valk et al. [17] using MEGNO and in Delsate et al. [6] and Lemaître et al. [11] using the FMA.

We remark the well-know double-pendulum 1:1 resonance due to  $C_{22}$ . We show the presence of the so-called additional resonances, associated, regarding the angle  $\sigma$ , with periods commensurate with 1 year. More precisely, the major additional resonance located at approximately 45-55 km on both sides of the pendulum-like pattern are related to a 2 years fundamental period of  $\sigma$ . Concerning the farther patterns located at  $\pm 80$  km, the fundamental period of  $\sigma$  turns out to be very close to 1 year. As a consequence, we can conclude that these additional resonances are actually related to a commensurability between  $\sigma$  and the 1 year period angle  $\lambda_S$ , that is the ecliptic longitude of the Sun. Our analysis suggests that other additional resonances can be observed. A first one when the period is equal to 3 years (at  $\pm 37$  km above the "eye") and a second resonance when the period is equal to 4 years (at  $-35$  km below the main resonance). We can also observe three islands of secondary resonances inside the "eye" of the resonance (due to  $C_{22}$ ) when the period of the resonant angle is equal to 3 years, close to the separatrix.

## 2.2. Analytical tools and results

The details about this analytical study can be found in Lemaître et al. [11].

The model is a pendulum-like, averaged over the short periodic terms and perturbed by the solar radiation pressure through the eccentricity.

We write the Hamiltonian  $\mathcal{H}$ , averaged over the short periodic terms and truncated, describing the space debris dynamics on a geostationary orbit:

$$\mathcal{H} = -\frac{\mu^2}{2L^2} - \dot{\theta}L + \frac{\mu}{a^3} R_e^2 \left( F_{200}(i) G_{200}(e) S_{2200} + F_{221}(i) G_{212}(e) S_{2212} \right)$$

in which  $\dot{\theta}$  is the angular velocity of the Earth ( $2\pi$  per day), the functions  $F$  and  $G$  are taken from the potential development of Kaula [7],  $R_e$  is the mean equatorial Earth's radius and  $\mu$  is the gravitational constant of the Earth.  $a$ ,  $e$  and  $i$  are the three first keplerian elements of the GEO space debris. We consider that  $i = 0$ . We introduce the resonant angle (1:1) of the geostationary orbit  $\sigma = \lambda - \theta$ . We rewrite  $S_{2200}$  as

$$S_{2200} = C_{22} \cos 2\sigma + S_{22} \sin 2\sigma = J_{22} \cos 2(\sigma - \sigma_0).$$

The variable  $\sigma$  is conjugated to  $L = \sqrt{\mu a}$  and the Hamil-

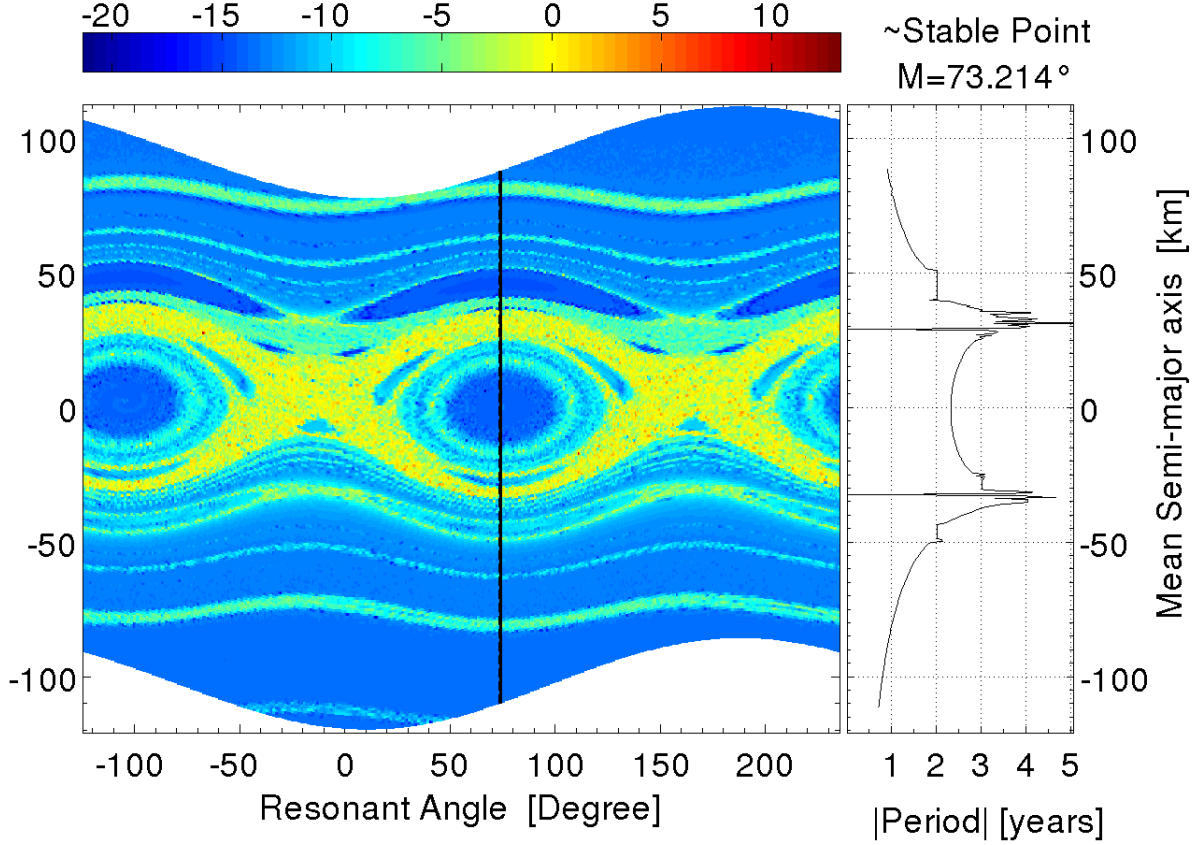


Figure 2. An atlas (with a simple model described in the text) of the estimate of the diffusion rate of the main frequency of the resonant angle for a near GEO space debris. A semi-major axis equal to 0 corresponding to 42 164.140 km.

tonian is now reduced to:

$$\mathcal{H} = -\frac{\mu^2}{2L^2} - \dot{\theta}L + \frac{3\mu^4}{L^6} R_e^2 J_{22} \cos 2(\sigma - \sigma_0) - \frac{15\mu^4}{2L^6} R_e^2 e^2 J_{22} \cos 2(\sigma - \sigma_0).$$

We introduce through  $e^2$  the second effect, caused by the solar radiation pressure. Indeed, Valk et al. [16] showed that, in presence of very large values of  $A/m$ , the motion of the eccentricity can be given by a simple expression, connecting the pericenter motion to the longitude of the Sun  $\lambda_S$  (associated to the corresponding frequency  $n_S = 2\pi$  per year). We shall consider the Sun on a circular orbit.

We make a last simplification by choosing the obliquity equal to 0.

$$e^2 = \frac{\mathcal{Z}^2}{L^2 n_S^2} + \gamma^2 + \frac{2\mathcal{Z}}{Ln_S} \gamma \cos(\lambda_S + \delta).$$

The Sun's initial conditions are given by  $\gamma$  and  $\delta$  and for the solar radiation pressure the parameter  $\mathcal{Z}$  is equal to

$\frac{3}{2} C_r P_r \frac{A}{m} a$  (see [16] for details). The final Hamiltonian  $K$  is:

$$K(L, \sigma) = -\frac{\mu^2}{2L^2} - \dot{\theta}L + \cos(2\sigma - 2\sigma_0) \left[ \frac{F}{L^6} - \frac{2G}{L^6} \cos(\lambda_S + \delta) \right], \quad \text{with}$$

$$F = 3\mu^4 R_e^2 J_{22} - \frac{15\mu^4}{2} R_e^2 J_{22} \left( \frac{\mathcal{Z}^2}{L^2 n_S^2} + \gamma^2 \right)$$

$$G = \frac{15\mu^4}{2} R_e^2 J_{22} \frac{\mathcal{Z}}{Ln_S} \gamma.$$

For the numerical integrations shown in Fig. 2, the initial conditions correspond to  $\delta = 0.8934$ ,  $n_S = -\frac{2\pi}{\text{year}}$ . Now, suitable action angle variables are introduced in the unperturbed pendulum, successively in the libration and in the circulation regions. The same canonical transformations are applied to the perturbation part, for both regions, and the new resonance models appear, after a last averaging process over periods of one year, to make appear, locally, very long periods of time. The introduction of these couples of action-angle variables allows us to detect all the significant resonances and their respective positions, to find the sizes of the small islands and to

give, for each of them, an adequate very local model of resonance.

With the help of these analytical representation, we find, for example, the periods of  $\sigma$  with respect to the semi-major axis for the circulation region (Fig. 3). We can see the possible localisation of the secondary resonances (when the period of  $\sigma$  is a multiple of one year). These results are in agreement with the numerical results (Fig. 2).

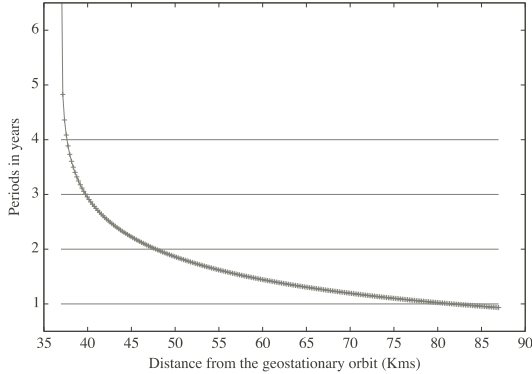


Figure 3. The periods of  $\sigma$  calculated in years, as functions of the distance (in kilometers) from the separatrix, calculated for, obtained analytically (line) and by a numerical integration of the pendulum differential equations (dots).

For the case of circulation, the resonances found analytically correspond to periods of the angle  $\sigma - \sigma_0$  of 2, 4 and 6 years; to find the odd periods (corresponding to 1 or 3 years), we have to use the more complete formula for the introduction of the second frequency through the eccentricity, with a nonzero obliquity. If we consider the most important resonance (2 years), with the analytical study, we obtain that this resonance is situated at 46 kms from the separatrix (in agreement with the numerical results in Fig. 2). A rough approximation gives the frequency and (minimal) period of this secondary resonance, for  $\frac{F}{G} \simeq 30$  as in the numerical simulations:  $T_2 \text{ years} \simeq 11 \text{ years}$ . This results agrees with the numerical integration [11].

For the libration case, the first resonance is characterized by a period of 3 years for  $\sigma$ ; it is described by the angle  $\Phi = 3\sigma - (\lambda_S + \delta)$ . The following resonances (4 or 5 years) are very close to the separatrix with a very small amplitude, and do not appear clearly on the numerical results (Fig. 4). They overlap to each other to create the chaotic layer around the separatrix. If we take only into account the terms corresponding to this 3:1 resonance, we can explain the location of the 3 islands of resonances (in the main eye of the resonance 1:1).

The three equilibrium islands are situated at  $\frac{2\pi}{3}, \pi$  and  $\frac{5\pi}{3}$ , which correspond to the values of  $\Phi - \frac{\delta + \lambda_{S_0}}{3}$ . Let us remind that  $\delta$  depends on the initial conditions in eccentricity and pericenter and is fixed to  $51.19^\circ$  for the refer-

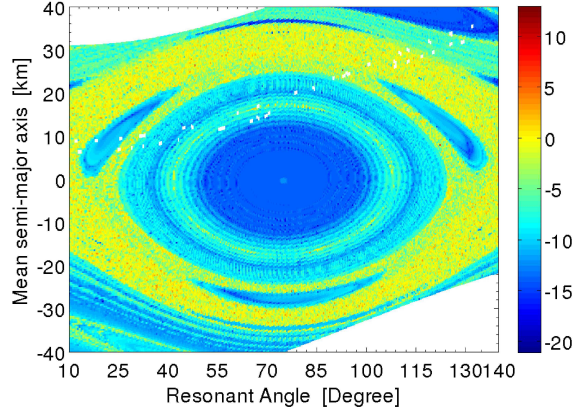


Figure 4. Numerical study. Blow-up around a stable point of the phase space of the Fig. 2.

ence simulations; the initial value of the Sun's longitude is  $\lambda_{S_0} = 128.01^\circ$ . The three values of  $\Phi$  are then

$$60.26^\circ, 180.26^\circ \text{ and } 300.26^\circ,$$

measured from the vertical positive axis in a frame centered on the stable point. The Fig. 4 (numerical FMA) confirms these results.

### 3. CONCLUSIONS

Using the numerical stability indicator (FMA), we brought into evidence a relevant class of additional resonances in the GEO for space debris with high area-to-mass ratios. We have first numerically analysed these resonances and we confirm and explain our results by an analytical study.

Our simplified model reproduces and explains the structure obtained by the MEGNO and by the FMA. The web of islands is clearly connected to secondary resonances between the geostationary resonant angle and the longitude of the Sun, present in the solar radiation pressure. The size of these islands is directly proportional to the coefficient  $A/m$  which is responsible for this web.

The next step is the study of potential captures of space debris into resonances. If the captures could be efficient for several years, these islands should be regions of particular interest to gather and concentrate debris for some times.

### ACKNOWLEDGMENTS

N. Delsate was welcomed by the IMCCE in Paris for the numerical part of this work; the authors would like to thank Ph. Robutel and J. Laskar for their efficient collaboration.

## REFERENCES

- [1] Anselmo, L., Pardini, C., 2005, In: Danesy, D. (Ed.), *Proceedings of the Fourth European Conference on Space Debris*, (ESA SP-587). ESA Publications Division, Noordwijk, The Netherlands, pp. 279–284.
- [2] Breiter, S., Wytrzyszczak, I., Melendo, B., 2005, *Advances in Space Research* 35, 1313–1317.
- [3] Chao, C. C., 2006, In: *Proceedings of the 2006 AIAA/AAS Astrodynamics Specialist Conference*. Keystone, Colorado, AIAA Paper, No. AIAA-2006-6514.
- [4] Cincotta, P. M., Simó, C., 2000, *Astronomy and Astrophysics*, Supplement 147, 205228.
- [5] Cincotta, P. M., Giordano, C. M., Simó, C., 2003, *Physica D* 182, 151178
- [6] Delsate, N., Valk, S., Carletti, T., Lemaître, 2008, *SF2A-2008: Proceedings of the Annual meeting of the French Society of Astronomy and Astrophysics*, Eds.: C. Charbonnel, F. Combes and R. Samadi. Available online at <http://proc.sf2a.asso.fr>, p.113.
- [7] Kaula, W.M., 1966, Blaisdell Publishing Company, Waltham Massachusetts, Toronto, London.
- [8] Laskar, J., 1990, *Icarus* 88, 266–291.
- [9] Laskar, J., 1993, *Physica D* 67, 257–281.
- [10] Laskar, J., 1995, *Proceedings of 3DHAM95 NATO Advanced Institute*. Vol. 533. S'Agaro, pp. 134–150.
- [11] Lemaître, A., Delsate, N., Valk, S., 2009, Accepted to *Celestial Mechanics and Dynamical Astronomy*.
- [12] Liou, J.-C., Weaver, J. K., 2004, *The Orbital Quarterly News* 8 issue 3, The NASA Orbital Debris Program Office.
- [13] Liou, J.-C., Weaver, J. K., 2005, In: Danesy, D. (Ed.), *Proceedings of the Fourth European Conference on Space Debris* (ESA SP-589). ESA Publications Division, Noordwijk, The Netherlands, pp. 285–290.
- [14] Schildknecht, T. et al., 2004, *Advances in Space Research* 34, 901–911.
- [15] Schildknecht, T. et al., 2005, In: Danesy, D. (Ed.), *Proceedings of the Fourth European Conference on Space Debris*, ESA SP-587. ESA Publications Division, Noordwijk, The Netherlands, pp. 113–118.
- [16] Valk, S., Lemaître, A., Anselmo, L., 2008, *Advances in Space Research* 41, 1077–1090.
- [17] Valk, S., Delsate, N., Lemaître, A., Carletti, T., 2008, *Advances in Space Research*, doi 10.1016/j.asr.2009.02.014.